Publisher source acknowledgment: https://doi.org/10.1039/d3dt00734k (final version)

ARTICLE

Cisplatin and Zoledronic acid: two drugs combined in a Pt(II) complex with potential antitumor activity towards bone tumors and metastases.

Received 00th January 20xx,
Accepted 00th January 20xx

DOI: 10.1039/x0xx00000x

Alessandra Barbanente,[a] Nicoletta Ditaranto,[a] Antonio Laghezza,[b] Paolo Tortorella,[b] Francesco P. Intini,[a] Concetta Pacifico,[a] Giovanni Natile,[a] Nicola Margiotta.[a,*]

Treatment of primary bone malignancies comprises surgery, radiotherapy, chemotherapy, and analgesics. Platinum-based chemotherapeutics, such as cisplatin, are commonly used for the treatment of bone cancer but, despite their success, outcomes are limited by toxicity and resistance. Recently, dinuclear Pt complexes with a bridging geminal bisphosphonate ligand proved to be endowed with selective accumulation in bone tumors or metastases leading to improved efficacy and reduced systemic toxicity. A further improvement could be expected by the use of a bisphosphonate ligand with intrinsic pharmacological activity such as Zoledronic acid (ZL). In the present work is reported the synthesis and full characterization of the dinuclear Pt(II) complex [{*cis*-Pt$(NH_3)_2$}$_2$(ZL)]HSO_4 which combines two drugs with antitumor activity, cisplatin and Zoledronic acid. Both drugs, individually, are already approved by the U.S. Food and Drug Administration and the European Medicinal Agency for clinical use. The *in vitro* cytotoxicity of the new Pt(II)-ZL complex has been tested against a panel of human tumor cell lines.

Introduction

Bone tumors develop when bone cells multiply without control, forming an unregulated mass. There are more than 30 types of primary bone cancers, the most common are the multiple myeloma and osteosarcoma for which the median survival time is six months in the absence of treatment[1]. Treatment of primary bone malignancies comprises surgery, radiotherapy, chemotherapy, and analgesics[2]. Bone metastases are the result of the progression of some other types of tumors; as an example prostate, breast, and lung cancers are most expected to spread to bones[3]. In fact, between 70 and 80% of patients with advanced breast or prostate cancer develop bone metastases[4,5] which can be divided in osteolytic (characterized by destruction of normal bone), osteoblastic (characterized by deposition of new bone), and mixed type (osteolytic/osteoblastic)[3]. Platinum-based chemotherapeutics, such as cisplatin, are commonly used for the treatment of bone cancer (these drugs induce cancer cell apoptosis by binding to DNA and forming Pt–DNA adducts)[6–9]. Despite its success, treatment with cisplatin is limited by undesirable side effects such as ototoxicity, nephrotoxicity, myelosuppression, and neurotoxicity[10,11]. These adverse effects could be minimized for drugs capable to go straight to their biological target (Drug Targeting and Delivery, DTD) so reducing systemic toxicity and overcoming resistance. A DTD strategy contemplates the choice of a carrier ligand that favors the accumulation of the drug in the target organs or cells[12–14]. Remarkable examples of potential carrier ligands are the bisphosphonate drugs (BPs) used as standard treatment for patients with malignant bone diseases, such as osteoporosis, Paget's disease, and tumor-induced osteolysis. BPs are endowed with high affinity for bones and other calcified tissues[15,16] and are known to be able to inhibit the osteoclast-mediated bone resorption[17]. Moreover, there is a growing body of evidence showing that BPs can also exhibit antitumor activity[18] by affecting molecular mechanisms of tumor cell adhesion, invasion, and proliferation[19]. Therefore, the combination of a BP with a platinum moiety could be promising for a selective accumulation of the platinum drug in bone-related tumors or metastases so improving the chemotherapeutic efficacy while reducing the systemic toxicity. Platinum(II) complexes with (aminoalkyl)phosphonic acids were first reported by Appleton[20,21] and subsequently exploited by Keppler and coworkes[22] that showed how Pt(II) complexes with amino-bis/tris(methylenephosphonate) ligands (ATMP and BPMAA, respectively) could have therapeutic activity superior to that of cisplatin in an orthotopically transplanted rat osteosarcoma model[23,24]. Other interesting Pt-BP compounds, like *cis*-[PtL$(NH_3)_2$Cl]NO_3 {BPP; L = tetraethyl [2-(pyridin-2-yl)ethane-1,1-diyl]bisphosphonate}, were reported by Guo and coworkers, displaying effective inhibitions against OS (Osteosarcoma) cells. In particular, they demonstrated that BP targeting group not only improves the selectivity of the platinum complex toward sarcoma cells but also reduces the systemic toxicity [25]. Recently, Margiotta et al. showed that the 2-ammonium-1-hydroxyethane-1,1-diyl-bisphosphonate and the 3-ammonium-1-hydroxpropane-1,1-diyl-bisphosphonate could act as a bridge between two [Pt(*cis*-1,4-DACH)]$^{2+}$ moieties. [Pt(*cis*-1,4-DACH)]$^{2+}$ is obtained by loss of the two

[a] *Dipartimento di Chimica, Università degli Studi di Bari Aldo Moro, Via E. Orabona 4, 70125 Bari, Italy;*
[b] *Dipartimento di Farmacia-Scienze del Farmaco, Università degli Studi di Bari Aldo Moro, Via E. Orabona 4, 70125 Bari, Italy.*
* Corresponding Author; email: nicola.margiotta@uniba.it
Electronic Supplementary Information (ESI) available: [details of any supplementary information available should be included here]. See DOI: 10.1039/x0xx00000x

chlorido ligands from kiteplatin ([$PtCl_2$(cis-1,4-DACH)], DACH = diaminocyclohexane) known to be able to overcome both the cisplatin and the oxaliplatin-resistance[26]. The obtained dimeric species [{Pt(*cis*-1,4-DACH)}$_2$(BP)]$^+$ were able to overcome the cisplatin-resistance and also to circumvent the multi-drug resistance in the colorectal cell line pair LoVo/LoVo-MDR[27]. Moreover, in another study they also demonstrated, by using radioactive BP-functionalized Pt complexes (^{195m}Pt-BP), systemically administered to mice, a 4.5-fold higher affinity to bone compared to platinum complexes lacking the bone-seeking bisphosphonate moiety[28]. The ^{195m}Pt-BP complex was able to specifically accumulate in intratibial bone metastases (7.3-fold more efficiently than ^{195m}Pt-cisplatin) and was radiotherapeutically more active (11-fold) than the non-radioactive Pt-BP analog[29]. Zoledronic acid is the most potent among the BPs and has been widely used in the clinic to prevent and treat skeletal-related events in patients affected by metastatic castration-resistant prostate cancer (mCRPC)[30]. Thus, Qiu et al. prepared different platinum complexes with imidazolyl-containing bisphosphonates which showed remarkable anticancer effect, on several cancer cell lines, caused by cell cycle arrest and apoptosis [31]. The same authors, more recently, showed that the supplementation of mevalonate pathway intermediate Farnesol can partly overcome the anticancer effects of [{*cis*-Pt(en)}$_2$(ZL)] (Chart 1) on SGC7901 cells by rescuing the cell cycle arrest and apoptosis, and the isoprenylation of small G proteins. These observations indicate that [{*cis*-Pt(en)}$_2$(ZL)] exerts the anticancer effect on SGC7901 cells by inhibiting the mevalonate pathway[32]. Encouraged by these positive results, and in the perspective of a possible clinic investigation, we have prepared the complex [{*cis*-Pt(NH_3)$_2$}$_2$(ZL)] (**1**, Chart 1) in which the antitumor drug cisplatin and Zoledronic Acid are combined together; it is worth of note that both individual drugs are already approved by the Food and Drug Administration and the European Medicinal Agency for clinical use. The Zoledronic ligand should ensure high tropism of the cisplatin-containing drug toward bone tumors. The synthesized new complex has been fully characterized and its chemical stability investigated in a physiological-like buffer as well as in acidic conditions to simulate the low-pH environment typically surrounding a tumor mass. The reactivity of **1** with 5'-GMP, used as the simplest model of DNA, was also investigated. Finally, the Pt(II) complex was tested to assess its in vitro cytotoxicity against a panel of human tumor cell lines.

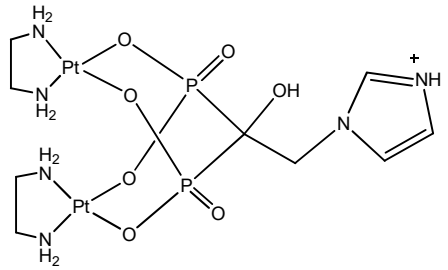

[{*cis*-Pt(en)}$_2$(ZL)]$^+$

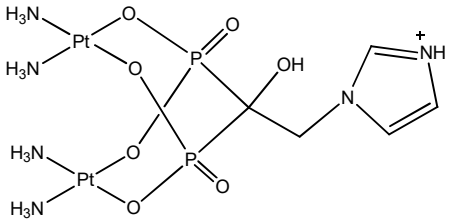

[{*cis*-Pt(NH_3)$_2$}$_2$(ZL)]$^+$ (1)

Chart 1: Sketches of the already reported [{*cis*-Pt(en)}$_2$(ZL)]$^+$ and the new [{*cis*-Pt(NH_3)$_2$}$_2$(ZL)]$^+$ dinuclear Pt-bisphosphonate complex (en = ethylenediamine, ZL = zoledronic acid).

Experimental section

Starting materials and instrument details

Commercial reagent-grade chemicals and solvents (Sigma, Milan, Italy) were used as received without further purification. 1D ^{1}H-, ^{31}P-, and ^{195}Pt-NMR and 2D [^{1}H-^{13}C]-HSQC and HMBC spectra were recorded on Bruker Avance DPX 300 MHz (Bruker Italia S.r.L., Milano, Italy) instrument. Standard pulse sequences were used for ^{1}H, ^{31}P{^{1}H}, and ^{195}Pt{^{1}H} (121.5, 242.9, and 64.5 MHz, respectively) one-dimensional spectra. ^{1}H chemical shifts were referenced using the internal residual peak of the solvent (D_2O: 4.80 ppm), ^{31}P chemical shifts were referenced to external H_3PO_4 (85% w/w; 0 ppm), while the ^{195}Pt chemical shifts were referenced to external $K_2[PtCl_4]$ in D_2O fixed at −1628 ppm. Electrospray ionization mass spectrometry (ESI-MS) was performed with a dual electrospray interface and a quadrupole time-of-flight mass spectrometer (Agilent 6530 Series Accurate-Mass Quadrupole Time-of-Flight (Q-TOF) LC-MS) (Agilent Technologies Italia S.p.A.; Cernusco sul Naviglio, Milano, Italy). Elemental analyses were performed with an Eurovector EA 3000 CHN instrument (Eurovector S.p.A., Milano, Italy). A Crison Micro- pH meter Model 2002, equipped with Crison micro-combination electrodes (5 and 3 mm in diameter) (Hach Lange Spain, S.L.U.; Barcelona, Spain) and calibrated with Crison standard buffer solutions at pH 4.01, 7.02, and 10.00, were used for pH measurements. The pH readings from the pH-meter for D_2O solutions are indicated as pH* values and are uncorrected for the effect of deuterium on glass electrodes[33].

Synthesis of bisphosphonic acid

1-Hydroxy-3-(1H-imidazol-1-yl)ethane-1,1-diylbisphosphonic acid, commonly known as zoledronic acid (ZL), was prepared according to an already reported procedure[34].

Synthesis of the platinum compounds

Cis-$[PtI_2(NH_3)_2]$[35] and *cis*-$[Pt(OSO_3)(OH_2)(NH_3)_2]$ were prepared as already reported[27]. The elemental analyses and the spectroscopic features of the Pt precursor complexes were consistent with the data reported in the literature.

Preparation of [{*cis*-Pt(NH$_3$)$_2$}$_2$(ZL)]HSO$_4$.

1-Hydroxy-3-(1H-imidazol-1-yl)ethane-1,1-diylbisphosphonic acid (ZL) (27.0 mg, 0.099 mmol) was dissolved in H_2O (6.7 mL) at 45 °C and treated with a solution of *cis*-$[Pt(OSO_3)(OH_2)(NH_3)_2]$ (75 mg, 0.218 mmol in 6.70 mL H_2O). The resulting solution was kept under stirring at 45 °C for 4 h, during which the pH was maintained at a constant value of ca. 4.0 by the addition of aliquots of KOH (1.0 M), as required. After concentration of the reaction solution to a volume of ca. 2 mL by rotary evaporation, the pH was lowered to ca. 2 by addition of H_2SO_4 (1M), and methanol was added to induce the precipitation of the desired product as a greenish solid having HSO_4^- as counterion. The precipitate was left standing at 4 °C for 10 minutes and then it was isolated by filtration of the solution, washed with methanol, and dried under vacuum. Obtained 52.3 mg (65% yield). Anal. Calcd. for [{*cis*-Pt$(NH_3)_2$}$_2$(ZL)]HSO_4·4H_2O ($C_5H_{19}N_6P_2O_{11}Pt_2S$ · 4H_2O): C, 6.70; H, 3.04; N, 9.38%. Found: C, 6.86; H, 3.02; N, 9.00%. ESI-MS: calc. for [{*cis*-Pt$(NH_3)_2$}$_2$(ZL)]$^+$, $[C_5H_{18}N_6O_7P_2Pt_2+H]^+$ *m/z* = 726.9989 ; Found: $[M+H]^+$ *m/z* = 727.0059. ^{1}H NMR (D_2O): 8.65 (1H, H3), 7.47 (1H, H2), 7.34 (1H, H1), 4.58 (2H, H4), 4.39 (12H, NH_3) ppm. ^{31}P NMR (D_2O): 34.50 ppm. ^{195}Pt NMR (D_2O): −1420.26 ppm. ^{31}C{^{1}H} NMR (D_2O): 138.71 (C3) 127.05 (C2), 121.08 (C1), 79.4 (C5), 54.43 (C4) ppm. See Figure 4 for numbering of atoms.

NMR experiment at different pH and calculation of the pKa values

Acidity constants were determined by ^{31}P and ^{1}H NMR chemical shift/pH* titrations. ZL (0.0073 mmol) and Pt compound (0.0024 mmol) were dissolved in 0.500 mL of D_2O and transferred into an NMR tube. The pH* of the sample was adjusted to the required value by addition of $DClO_4$ (10, 1.0, 0.5, 0.1, or 0.05 M) or NaOD (1.0, 0.5, 0.1, or 0.05 M) solutions, and the pH* value was measured by using a 3 mm diameter electrode for NMR tubes. No control of the ionic strength was performed. The pH titration curves were fitted to the Henderson−Hasselbalch equation using the program KaleidaGraph (version 3.5, Synergy Software, Reading, PA, USA)[36] and GraphPad Prism 7.0.

Study of chemical stability of complex 1 in the solid state by XPS

X-ray Photoelectron Spectroscopy (XPS) analyses were run on a PHI 5000 Versa Probe II Scanning XPS Microprobe spectrometer (ULVACPHI Inc.). Measurements were carried on using a monochromatic Al Kα source (large area mode, X-ray spot 100 µm) at a power of 99.9 W. Wide scans and detailed spectra (C1s, N1s, O1s, Cl2p, Na1s, P2p, Pt4f) were acquired in Constant Analyzer Energy (CAE) mode with a pass energy of 117.40 and 29.35 eV, respectively. An electron gun was used for charge compensation (1.0 V 20.0 µA). Data processing was performed by using the MultiPak software v. 9.8.0.19.

Stability in Physiological or Acidic Conditions

The stability of the Pt-compound at 37 °C in buffered solutions was assessed by ^{31}P NMR spectroscopy. The Pt complex (~2 mg) was dissolved in 0.8 mL of D_2O containing 50 mM 4-(2-hydroxyethyl)-1-piperazineethanesulfonic acid) (HEPES) buffer (pH* = 7.4 or 6.5) and 120 mM NaCl. The resulting solutions were transferred into NMR tubes and maintained at 37 °C. ^{31}P NMR spectra were recorded from time to time over a period of 7 days.

Reactivity with 5'-GMP

Complex 1 (2mg, 0.0025 mmol) was dissolved in 0.8 mL of D_2O containing 50 mM HEPES buffer (pH*=7.4) and 120 mM NaCl to simulate the extracellular environment. After addition of 4.5 mg (0.011 mmol) of guanosine 5'-monophpsphate sodium salt (5'-GMP-Na·6H_2O), the reaction mixture was transferred into an NMR tube that was maintained at 37 °C. The reaction was monitored up to 7 days by recording ^{1}H and ^{31}P NMR spectra at defined time intervals.

In vitro cytotoxicity

The number of living cells was evaluated by the 3-(4,5-dimethylthiazol-2-yl)-2,5-diphenyltetrazolium bromide (MTT) assay. Cells were seeded at a density of ≈15000 cells/well into 96-well flat bottom culture plates containing 50 µL of the test compounds (ranged from 1 mM to 100 nM final concentration) in a final volume of 100 µL. Untreated cells were used as positive controls. After 48 h of incubation at 37 °C in a 5% CO_2 atmosphere, 3-(4,5-dimethylthiazol-2-yl)-2,5-diphenyltetrazolium bromide (MTT) was added to a final concentration of 0.5 mg/mL. Background absorbance was measured in six wells of cells, which were lysed with Triton X-100 (0.1% v/v final concentration) immediately prior to the addition of MTT reagent. After incubation under the same conditions for a further 3−4 h, the culture medium was removed, and the insoluble product was dissolved by the addition of 100 µL of solvent (1:1 v/v DMSO/EtOH). The absorbance of each well was measured at 570 nm using a Perkin-Elmer Victor V3 plate reader. Cell growth inhibition was then calculated as a percentage of cell viability relative to the control and IC_{50} values were determined from dose−response curves using GraphPad PRISM version 5.0.

Results and Discussion

Synthesis and characterization of the bisphosphonate

Zoledronic acid (1-hydroxy-3-(1H-imidazol-1-yl)ethane-1,1-diylbisphosphonic acid, ZL) was synthesized according to a procedure already reported in the literature[34] and was characterized by elemental analysis and 1D (^{1}H and ^{31}P) and 2D (COSY, [^{1}H,^{13}C]-HSQC, and [^{1}H,^{13}C]-HMBC) NMR experiments. The ^{1}H NMR spectrum of ZL in D_2O shows three singlets at 7.28, 7.43, and 8.62 ppm, and a multiplet at 4.58 ppm (H_1, H_2, H_3, and H_4, respectively). The cross-peaks linking the signals at 7.28 and 7.43 ppm (C in the COSY spectrum reported in Fig.1 A) testifies the strong correlation between protons H_1 and H_2; which, therefore, must belong to adjacent CH. The [^{1}H,^{13}C]-HSQC spectrum (Fig.1C) allowed the assignment of the resonances to

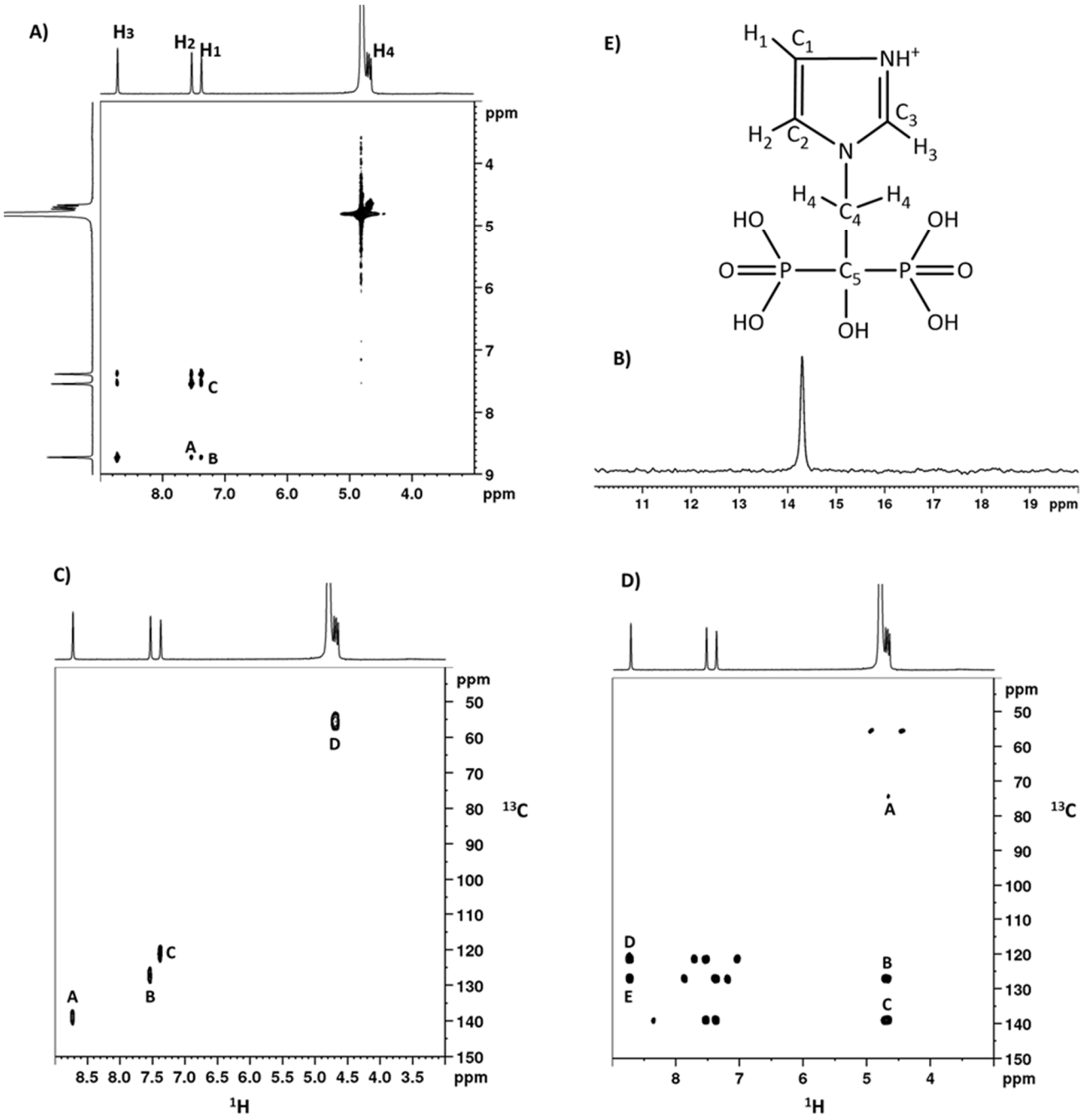

Figure 1: A) COSY (300 MHz), B) $^{31}P\{^{1}H\}$ (121.5 MHz), C) [^{1}H-^{13}C] HSQC (75.5 MHz, ^{13}C), and, D) [^{1}H-^{13}C] HMBC (75.5 MHz, ^{13}C), of Zoledronic Acid in D_2O (pH* = 1.90). E) Numbering of atoms.

the carbon atoms to which the protons are bound. Thus, cross peaks ($^{13}C/^{1}H$) falling at 138.88/8.62 (A), 127.08/7.43 (B), 120.96/7.28 (C), and 55.38/4.58 ppm (D) assign the resonances at 120.26, 127.08, 138.88, and 55.38 to C_1, C_2, C_3, and C_4, respectively. The resonance of the quaternary C_5 carbon atom, could be assigned by recording the 2D HMBC NMR spectrum (Fig. 1D) in which the cross peak (A) testifies the presence of a long range coupling between H_4 (4.58 ppm) and a carbon atom (C_5) resonating at 74.22 ppm. The 2D HMBC NMR spectrum also shows that H_4 is linked with cross peaks to C_2 and C_3 (B and C in Fig. 1D) but not to C_1, therefore C_2 and C_3 are closer to H_4 than C_1; in addition, cross peaks D and E correlating H_3 with C_1 and C_2, assign the latter two to the adjacent carbon atoms. The $^{31}P\{^{1}H\}$-NMR spectrum (Fig. 1B) shows a singlet falling at 14.17 ppm (assigned to the two equivalent P atoms), the chemical shift is that typical of a geminal bisphosphonate[27,37,38].

The pK_a values of various deprotonation steps of ZL were obtained by recording ^{1}H and $^{31}P\{^{1}H\}$-NMR spectra at different pH* values. The plot of the ^{31}P chemical shift as a function of pH* is given in Fig. 2A. The titration curve shows four inflection points corresponding to the various deprotonation steps of ZL (Scheme 1). As the pH of the sample was increased from ca. 0.38 to 2 we observed a shift to higher field of the ^{31}P chemical shift with an inflection point (calculated by fitting the points between pH 0.38 and 2 to the Henderson–Hasselbalch equation)[36] falling

at pH=1.25. This value corresponds to the pK_a of the second deprotonation step (pK_{a2} in scheme 1) since the first deprotonation step occurs at lower pH. It is known that deprotonation of an OH in a bisphosphonate shields the phosphorous nucleus directly attached to it ("direct effect") and deshields the distant second phosphorous atom ("remote effect")[21]. In this case, the direct effect prevails on the remote effect and so the global result is a shielding of the phosphorous nuclei. By further increasing the pH from 2 to 4 a second inflection point is observed which falls at pH=2.32 and is assigned to the third deprotonation step (pK_{a3}, Scheme 1). Further increase of the pH from 4 to 8 caused a huge deshielding of the phosphorous nuclei with an inflection point falling at pH = 7.38 which corresponds to pK_{a4}. In order to determine the value of pK_{a5} we took advantage of the ^{1}H NMR chemical shift of the imidazole protons whose plot is reported in Fig.2B. The three curves have been fitted to the Henderson-Hasselbalch equation affording very close inflection points at 8.01, 7.99, and 7.96 for H_1, H_2, and H_3, respectively, which can be averaged to a pKa value of 7.99. The remaining pKa value (pK_{a6}) could be derived from the ^{31}P titration curve. By increasing the pH from 8 to 14 we observed an inflection point falling at 12.08 which, most likely, corresponds to the deprotonation of the hydroxylic group bound to the central carbon. It is to be noted that the experimental pK_a values are quite different from those which can be calculated using the software ACD pKa LABS suite ver. 10.01 (Table1, SI), further confirming that, when possible, it is better to rely on experimental values than on simulated data.

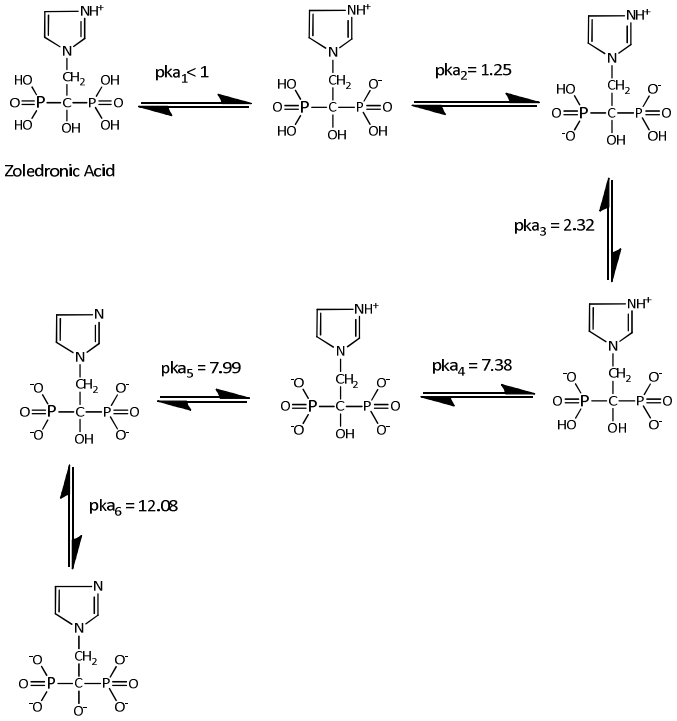

Scheme 1

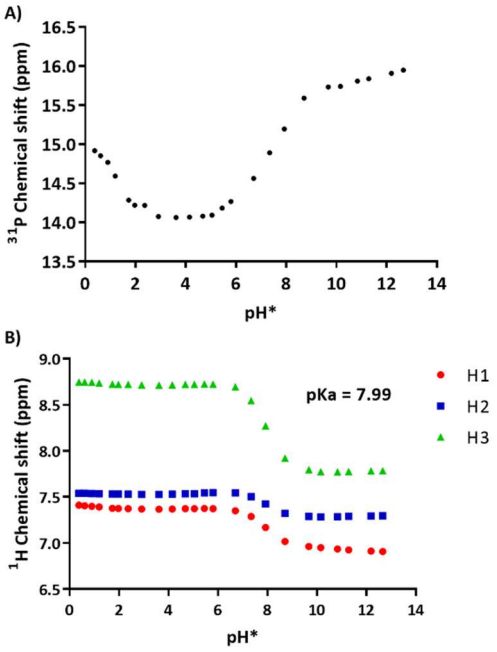

Figure 2: Plot of ^{31}P (A) and ^{1}H (B) chemical shift *vs.* pH* for Zoledronic Acid.

Synthesis and characterization of the dinuclear platinum complex

The synthesis of the dinuclear complex [{*cis*-Pt$(NH_3)_2$}$_2$(ZL)]HSO_4 was performed using two equivalents of *cis*-[Pt$(OSO_3)(OH_2)(NH_3)_2$] and one mole equivalent of zoledronic acid (ZL). With the aim of investigating the mechanism of formation of complex **1**, we recorded ^{1}H- and ^{31}P-NMR spectra at different time intervals (Fig. 3). The ^{31}P NMR spectrum, recorded soon after mixing of the reactants, shows, apart from the signal of free ZL (marked with a full circle in Fig 3B), two less shielded signals falling at 23.29 and 34.50 ppm. Based on literature data[39], the signal at 23.29 ppm (marked with a full star) can be assigned to a mononuclear Pt-ZL derivative, while the signal at 34.50 ppm (marked with a full triangle) can be assigned to the dinuclear complex **1** (in both cases the bisphosphonate is symmetric). With time, the intensity of the signal of monomeric Pt-ZL decreases with the simultaneous increase of the signal of the dinuclear species at 34.50 ppm. The coordination of BP to Pt determined an acidification of the reaction solution, thus after 6h the pH was brought to 4 by addition of KOH in order to bring the reaction to completion. The formation of complex **1** was also monitored by ^{1}H NMR spectroscopy (Fig. 3C). In this case only two sets of signals were observed, one close to that of free ZL and the other corresponding to the final dinuclear complex **1**, we can conclude that the ^{1}H signals of the monomeric Pt-ZL species are close to and overlapping with those of free ZL. As matter of fact, the signals of the final complex **1** (8.65, 7.47, and 7.34 ppm) are only slightly more shielded with respect to those of free ZL (and the monomeric form). It is possible to conclude that the formation of complex **1** contemplates an intermediate mononuclear Pt species with symmetric bisphosphonate [*cis*-Pt$(NH_3)_2$(ZL)]$^+$ (Pt-ZL) which can then react with a second Pt residue to afford the

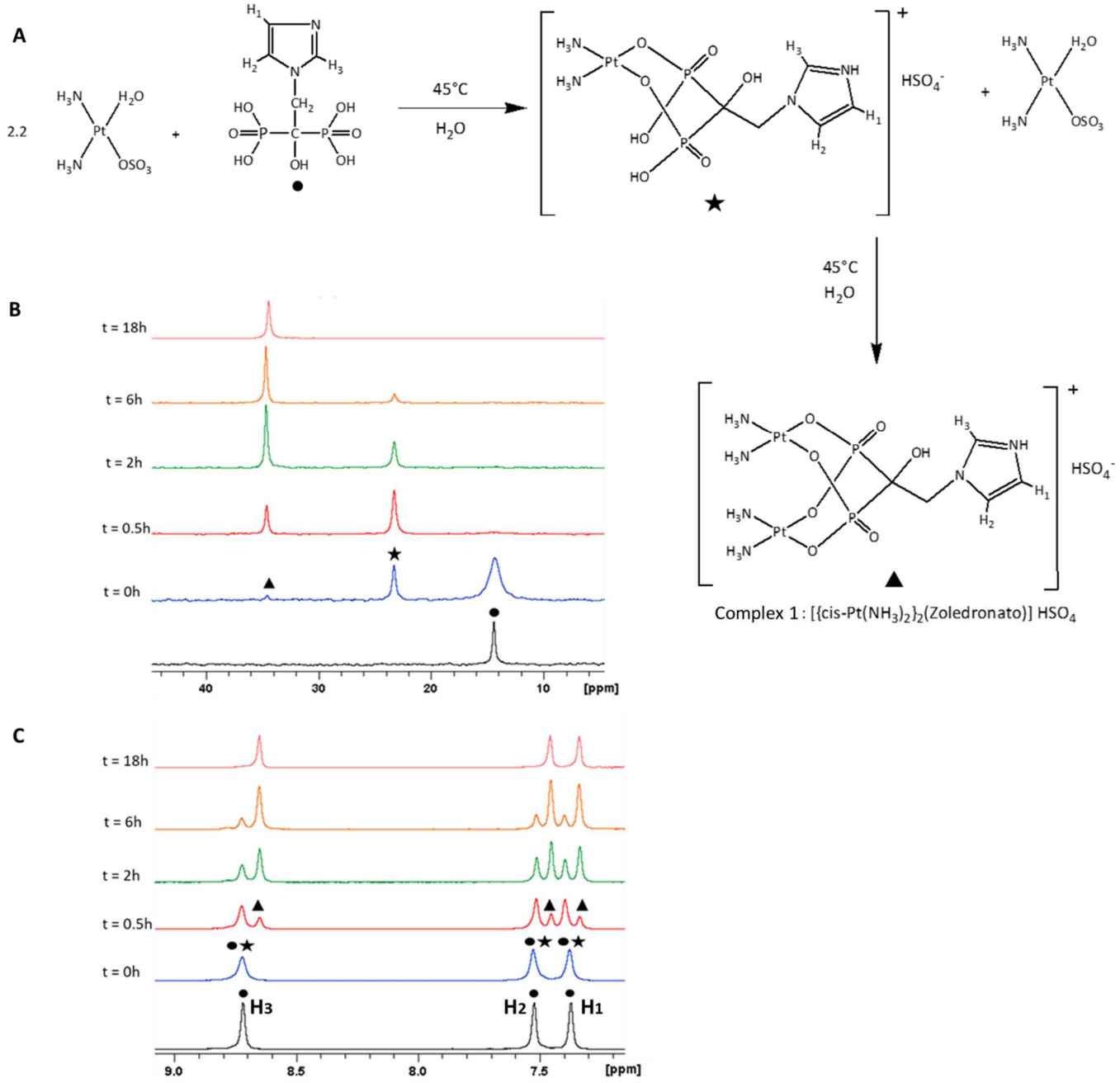

Figure 3: A) Scheme of the mechanism of formation of complex **1**. (B) ^{31}P- and (C) ^{1}H- NMR spectra of the reaction mixture in D_2O recorded at different time intervals.

dinuclear complex **1**. Complex **1** was characterized by elemental analysis, ESI-MS, and 1D (^{1}H, ^{31}P, and ^{195}Pt NMR) and 2D ([^{1}H,^{13}C]-HSQC and [^{1}H,^{13}C]-HMBC) NMR. The elemental analysis of **1** was in accordance with the presence, in the molecule, of one zoledronate and two *cis*-$[Pt(NH_3)_2]^{2+}$ residues, as also confirmed by the ESI-MS spectrum showing a peak at *m/z*=727.0059 corresponding to $[\mathbf{1}+H]^+$ whose experimental isotopic pattern was in good agreement with the theoretical one (ESI, Fig. S1). The ^{1}H NMR spectrum of **1** in D_2O (Fig. 4A) shows three singlets at 8.65, 7.47, and 7.34 ppm, (H_3, H_2, and H_1, respectively) and a multiplet at 4.58 ppm, partially overlapping with the solvent signal (H_4). Finally, a broad signal falling at 4.39 ppm is assigned to the protons of the amminic ligands (NH_3). The ^{31}P{^{1}H}-NMR spectrum (Fig. 4B) shows a singlet falling at 34.50 ppm assigned to the two phosphorus atoms of the bisphosphonate group, which are magnetically equivalent and shifted to lower field ($\Delta\delta$ = 20.33 ppm) with respect to corresponding signal of the free ligand. Such a downfield shift of the phosphorus nuclei is characteristic of deprotonated phosphonate groups coordinated to a metal ion [21]. The ^{195}Pt-NMR of **1** (Fig. 4C) shows a very broad signal falling at –1418 ppm. The broadness of the Pt signal can be explained based on the peculiar structure of complex **1** and of analogous Pt-Bisphosphonate dinuclear complexes. In these complexes the bisphosphonate unit bridges the two platinum residues in a W conformation and the resulting structure has a plane of symmetry passing through the two Pt atoms and the phosphonate carbon atom (the P–C–P carbon atom), as a consequence the two phosphorous atoms are magnetically equivalent and only one signal is observed in the ^{31}P{^{1}H} NMR

spectrum. In contrast, the absence of a plane of symmetry passing through the P–C–P atoms (due to the presence of two different substituents on the central carbon atom: i.e. –OH and –CH_2–imidazole) renders the two platinum atoms magnetically unequivalent and two signals are observed in the ^{195}Pt NMR spectrum[27,37,38,40,41]. However, in the present case the two Pt atom have rather similar chemical shifts and a single broad signal is observed. Complex **1** was also characterized by a [^{1}H,^{13}C]-HSQC spectrum (Fig. 5A) which assign carbon atoms:

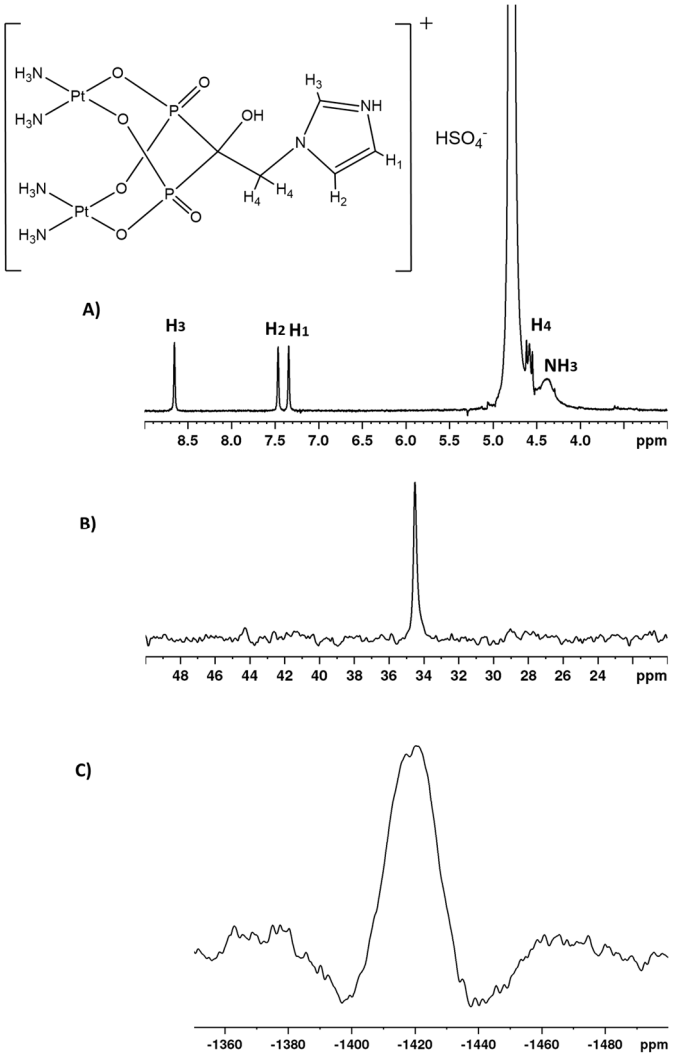

Figure 4: (**A**) ^{1}H NMR (300 MHz), (**B**) ^{31}P{^{1}H} (121.5 MHz), and (**C**) ^{195}Pt{^{1}H} (64.5 MHz) NMR spectra of **1** in D_2O.

the cross peaks falling at 138.71 (A), 127.05 (B), and 121.08 (C) ppm to the carbon atoms linked to H_3, H_2, and H_1, respectively, and the cross peak at 54.43 ppm (D) to the carbon atom linked to H_4. Finally, the 2D [^{1}H,^{13}C]-HMBC NMR spectrum (Fig. 5B) shows the cross peak A, falling at 4.58/79.4 ppm, correlating H_4 with C_5; cross peaks B and C correlating H_4 with C_2 and C_3, which assign C_2 and C_3 to the carbon atoms flanking the N atom; and cross peaks D and E correlating H_3 with C_1 and C_2, which assign the latter two to the adjacent carbon atoms.

The acid dissociation constant of complex **1** was determined by ^{1}H and ^{31}P{^{1}H}-NMR experiments at different pH*. The plots of the ^{31}P and ^{1}H chemical shifts as a function of pH* are given in Fig. 6 and show only one inflection point corresponding to the

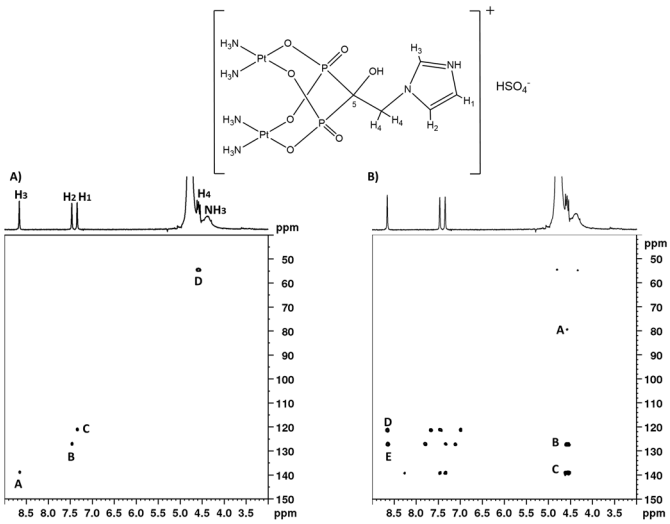

Figure 5: [^{1}H-^{13}C] HSQC (A) and HMBC (B) (75.5 MHz, ^{13}C) spectra of 1 in D_2O.

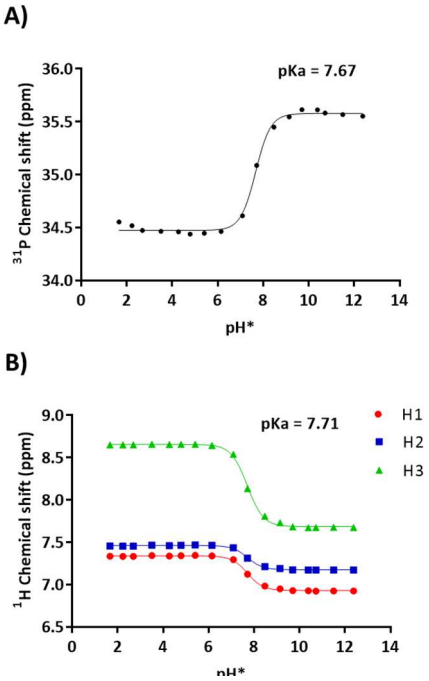

Figure 6: Plot of ^{31}P (A) and ^{1}H (B) chemical shift *vs.* pH* for complex **1**.

deprotonation of the imidazole nitrogen. By fitting the H_1, H_2, and H_3 titration curves was obtained a mean inflection point falling at 7.71, very close to the value obtained by fitting ^{31}P titration curve (7.67). This result confirms that all P-bound oxygens are coordinated to platinum atoms, and therefore cannot undergo neither protonation nor deprotonation.

Study of solid state chemical stability by XPS

Complex **1**, in the solid state, undergoes a slow color change from greenish to blue over time which was investigated by x-ray Photoelectron Spectroscopy (XPS). Curve fitting of the Pt4f XP spectrum resulted in two doublets (Figure 7a); the more abundant doublet has BE values ascribable to Pt(II) (Pt4$f_{7/2}$ =

72.9 ± 0.2 eV)[42], while the second, less abundant, doublet has at BE Pt4f$_{7/2}$ of 74.3 ± 0.2 eV which is higher than BE of Pt(II) but lower than the usual value of Pt(IV) (BE Pt4f$_{7/2}$ = 75.7 ± 0.2 eV). After 7 months aging the intensity of the second doublet (Figure 7b), increased from 11±1% to 17±1%. Based on the BE value[43] (in between those of Pt(II) and Pt(IV)) this doublet can be assigned to a Pt(III) species analogous to other dinuclear Pt(III) species previously prepared and characterized by some of us [44] (Figure S2). It is to be noted that Pt(III) species have been found as component of some intensely blue-coloured polymeric material named "platinblau"[45]. Starting from a dinuclear Pt(II) compound, the reaction leading to a dinuclear Pt(III) species can occur through removal (by an oxidant) of two electrons from a Pt(II) unit formally becoming Pt(IV). This process must be assisted by a ligand (a base) entering the coordination sphere of the Pt atom undergoing oxidation from the opposite side. In the case of dinuclear platinum species such as compound **1**, the second Pt(II) unit can act as a base contributing two d_z^2 electrons and binding along the axial direction in a face-to-face fashion [46]. The resulting dimer would be a formally Pt(III) species.

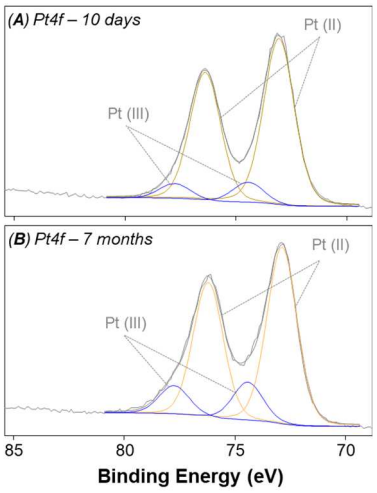

Figure 7: Curve-fitted Pt4f XP spectrum of complex **1** after 10 days (A) and 7 months (B).

Stability in Physiological and acidic Conditions

To investigate the stability of **1** in physiological and acid conditions resembling those observed in the extracellular matrix of tumors, D_2O solutions containing HEPES buffer (50 mM, pH*=7.4 or pH*=6.5) and NaCl (120 mM) were monitored at 37 °C by ^{31}P NMR spectroscopy. As can be seen from Figure 8, at pH*=7.4 and 37 °C, after 24 h there is, in addition to the signal of the starting compound **1** (34.50 ppm, marked with a full triangle) only a tiny new singlet falling at 23.29 ppm (marked with a full star) which further increases to nearly 30% of the total phosphorous after 72 h. The singlet at 23.29 ppm is indicative of a symmetric bisphosphonate and can be assigned to a mononuclear Pt-ZL species obtained by release of a *cis*-$[Pt(NH_3)_2]^{2+}$ moiety from **1**. No signal assignable to free ZL could be detected (singlet at 14.17 ppm). At more acidic pH* (6.5) and 37 °C, the ^{31}P-NMR spectrum shows after 24 h reaction the formation of the same singlet at 23.29 ppm (marked with a full star) assigned to a monomeric Pt-ZL complex. This signal also grows with time and after 72 h represents about 28% of the total phosphorous while no signal assignable to free ZL can be detected. It can be concluded that the behavior of **1** is very similar at pH 7.4 and 6.5.

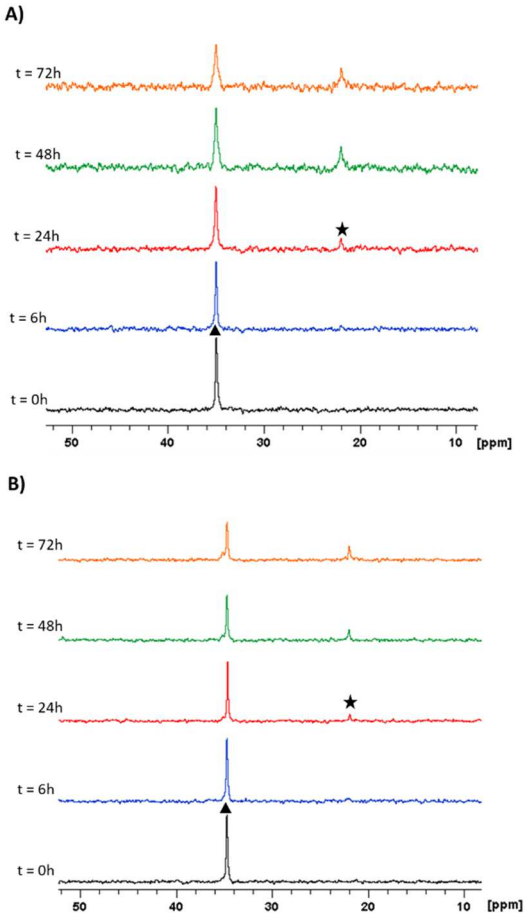

Figure 8: ^{31}P NMR (121.5 MHz) spectra at different times of **1** in physiological (A) and acidic (B) conditions (D_2O, HEPES buffer 50 mM, pH* = 7.4 or 6.5, 120 mM NaCl, 37 °C).

Reactivity with 5'GMP

The reaction of complex **1** with 5'GMP (4.5 equivalents, 0.011 mmol), as the simplest model of DNA, was investigated in 50 mM HEPES buffer (pH*=7.4) and 120 mM NaCl at 37°C by ^{31}P and ^{1}H NMR. The ^{31}P spectrum, recorded soon after mixing of the reactants, showed only the peaks belonging to free 5'-GMP (3.83 ppm; full circle in Fig. 9B) and starting Pt(II) complex (34.82 ppm; full triangle in Fig. 9B). After 72 h, it could be detected a new peak at 4.02 ppm (full diamond in Fig. 9B) which can be confidently assigned to the *cis*-$[Pt(5'\text{-GMP})_2(NH_3)_2]$ adduct[47] in addition to a tiny peak at 22.01 ppm belonging to the mononuclear Pt-ZL species (full star in Fig. 9B). The former peak grows with time, while the signal associated to complex **1** decreases. No signal assignable to free ZL could be detected. Moreover, a white opalescence was observed in the NMR tube; this was most likely due to precipitation of the monuclear Pt-ZL species under the experimental conditions used in our experiment. The low intensity of the ^{31}P NMR signal at 22.01 ppm is an evidence in support of our hypothesis. Therefore, this study highlighted that complex **1** react with 5'-GMP forming the mononuclear Pt-bisphosphonate intermediate *cis*-

$[Pt(NH_3)_2(ZL)]^+$ (Pt-ZL) and the bis-guanotide *cis*-$[Pt(5'\text{-}GMP)_2(NH_3)_2]$ complex by reaction of the released *cis*-$[Pt(NH_3)_2]^{2+}$ with 5'GMP (see Scheme of reaction in Fig.9A).

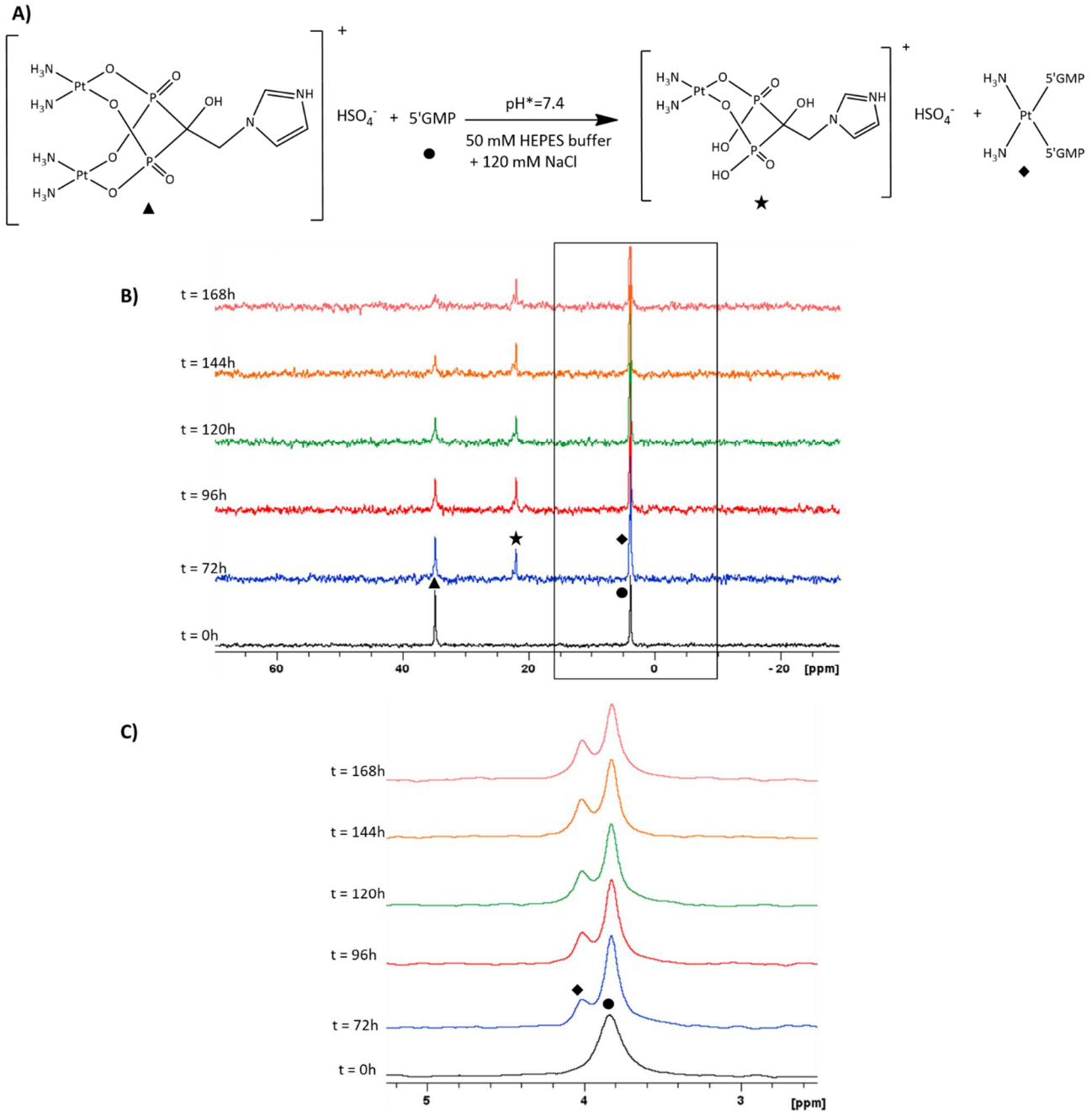

Figure 9: A) Scheme of the reaction of complex **1** with 5'GMP. B) ^{31}P NMR spectra of the reaction mixture at different time intervals. C) Magnification of the box indicated in B).

In vitro cytotoxicity

The in *vitro* cytotoxicity of complex **1** has been evaluated on a panel of human cancer cell lines which includes U937 (histiocytic lymphoma), HepG2 (liver), MCF-7 (breast), and MIA PaCa-2 (pancreas). Under the same experimental conditions were evaluated also cisplatin and zoledronic acid, the two pharmacologically active species combined in complex **1**. The cell viability was evaluated by means of the MTT test after 48 h of incubation with different concentrations of drug; the IC_{50} values, calculated from dose-survival curves, are reported in Table 1. The cytotoxicity of **1** is higher than that of the corresponding ligand (ZL) except against the HepG2 cell line. In particular, complex **1** showed an average IC_{50} of 159 µM and showed the best cytotoxicity towards the U937 cancer cell line (IC_{50} of 9.0 µM). The conjugation of cisplatin with zoledronic acid appears to improve the anticancer efficacy of the

bisphosphonate, but no that of cisplatin. In fact cisplatin was found to be the most effective compound towards all cell lines (average IC_{50} of 43.2 μM) most likely because of a faster substitution of the two chlorido ligands of cisplatin with respect to the zoledronate ligand of compound **1**.

Compounds	HepG2	MCF-7	U937	MIA PaCa-2
1	152±17	259±44	9.0±0.8	215±70
Zoledronic acid	57±14	>1000	>1000	>1000
Cisplatin	15.7±2.4	110±24	0.62±0.03	46.6±12.4

Table 1. Antiproliferative activity (IC_{50}, μM) obtained by the MTT test after 48 h of incubation with different concentrations of the tested compounds. Data are expressed as mean ± standard deviation (SD) of three independent experiments each performed in triplicate.

Conclusions

A new platinum compound having a dinuclear structure with a deprotonated Zoledronic acid bridging two *cis*-$[Pt(NH_3)_2]^{2+}$ moieties has been synthesized and fully characterized. The analytical and spectroscopic data support the complete loss of the phosphonate acidic protons with each phosphonate group bridging the two Pt atoms in a W conformation; as a consequence the two phosphorous atoms are magnetically equivalent while the two Pt atoms are not. ^1H and $^{31}P\{^1H\}$ NMR experiments at different pH values allowed to determine the acidity constants for free ZL and for complex **1**. The stability of complex **1** was found to be similar in physiological and acidic conditions (the latter characteristic of the tumor sites). Compound **1** reacts slowly with 5'-GMP (used as the simplest model of DNA) affording the bis-guanotide adduct *cis*-$[Pt(5'\text{-}GMP)_2(NH_3)_2]$. The *in vitro* cytotoxicity of the new compound was evaluated towards a set of 4 human tumor cell lines. Compound **1** was less cytotoxic than cisplatin but more cytotoxic than free zoledronate ZL and had the greatest activity towards the histiocytic lymphoma cell lines U937. It will be necessary to carry on an *in vivo* antitumor experiment to see if there is a specific targeting of the platinum drug to bone tumors promoted by the presence of the zoledronic ligand. The high solubility in water of complex **1** renders this compound also amenable to loading into inorganic matrices to be used as bone-fillers and reservoir of Pt-based drugs. Finally, a notable advantage of this new complex is the use of two clinical drugs that have already obtained approval from the U.S. Food and Drug Administration and European Medicinal Agency for their clinical use.

Acknowledgements

The authors are grateful to Alessia Dinoia (University of Bari, Italy) for the synthesis of Pt compounds. The University of Bari Aldo Moro and the Consorzio Interuniversitario di Ricerca in Chimica dei Metalli nei Sistemi Biologici (CIRCMSB) are gratefully acknowledged.

Conflicts of interest

There are no conflicts to declare.

References

1 J. Drach, H. Kaufmann, E. Urbauer, S. Schreiber, J. Ackermann and H. Huber, *J. Cancer Res. Clin. Oncol.*, 2000, **126**, 441–7.

2 H. Welkerling, T. Dreyer and G. Delling, *Virchows Arch. A Pathol. Anat. Histopathol.*, 1991, **418**, 419–425.

3 F. Macedo, K. Ladeira, F. Pinho, N. Saraiva, N. Bonito, L. Pinto and F. Gonçalves, *Oncol. Rev.*, 2017, **11**, 321.

4 L. Thibaudeau, V. M. Quent, B. M. Holzapfel, A. V Taubenberger, M. Straub and D. W. Hutmacher, *Cancer Metastasis Rev.*, 2014, **33**, 721–35.

5 M. van Driel and J. P. T. M. van Leeuwen, *Arch. Biochem. Biophys.*, 2014, **561**, 159–66.

6 E. J. Anthony, E. M. Bolitho, H. E. Bridgewater, O. W. L. Carter, J. M. Donnelly, C. Imberti, E. C. Lant, F. Lermyte, R. J. Needham, M. Palau, P. J. Sadler, H. Shi, F.-X. Wang, W.-Y. Zhang and Z. Zhang, *Chem. Sci.*, 2020, **11**, 12888–12917.

7 M. A. Jakupec, M. Galanski, V. B. Arion, C. G. Hartinger and B. K. Keppler, *Dalt. Trans.*, 2008, 183–194.

8 R. C. Todd and S. J. Lippard, *Metallomics*, 2009, **1**, 280.

9 D. Gibson, *Dalt. Trans.*, 2016, **45**, 12983–12991.

10 H. Uchino, Y. Matsumura, T. Negishi, F. Koizumi, T. Hayashi, T. Honda, N. Nishiyama, K. Kataoka, S. Naito and T. Kakizoe, *Br. J. Cancer*, 2005, **93**, 678–87.

11 V. A. Carozzi, P. Marmiroli and G. Cavaletti, *Curr. Cancer Drug Targets*, 2010, **10**, 670–682.

12 T. C. Johnstone, K. Suntharalingam and S. J. Lippard, *Chem. Rev.*, 2016, **116**, 3436–3486.

13 X. Wang and Z. Guo, *Chem. Soc. Rev.*, 2013, **42**, 202–224.

14 E. Gabano, M. Ravera and D. Osella, *Curr. Med. Chem.*, 2009, **16**, 4544–4580.

15 R. G. G. Russell, *Bone*, 2011, **49**, 2–19.

16 A. Lipton, *Expert Opin. Pharmacother.*, 2011, **12**, 749–762.

17 P. Clézardin, F. H. Ebetino and P. G. J. Fournier, *Cancer Res.*, 2005, **65**, 4971–4974.

18 J. R. Green, *Oncologist*, 2004, **9**, 3–13.

19 M. T. Drake, B. L. Clarke and S. Khosla, *Mayo Clin. Proc.*, 2008, **83**, 1032–1045.

20 T. G. Appleton, J. R. Hall and I. J. McMahon, *Inorg. Chem.*, 1986, **25**, 720–725.

21 T. G. Appleton, J. R. Hall and I. J. McMahon, *Inorg. Chem.*, 1986, **25**, 726–734.

22 T. Klenner, P. Valenzuela-Paz, B. K. Keppler, G. Angres, H. R. Scherf, F. Wingen, F. Amelung and D. Schmähl, *Cancer Treat. Rev.*, 1990, **17**, 253–259.

23 T. Klenner, F. Wingen, B. K. Keppler, B. Krempien and D. SchmÄhl, *J. Cancer Res. Clin. Oncol.*, 1990, **116**, 341–350.

24 T. Klenner, P. Valenzuela-Paz, B. K. Keppler and H. R. Scherf, *J. Cancer Res. Clin. Oncol.*, 1990, **116**, 453–458.

25 Z. Zhang, Z. Zhu, C. Luo, C. Zhu, C. Zhang, Z. Guo and X. Wang, *Inorg. Chem.*, 2018, **57**, 3315–3322.

26 N. Margiotta, C. Marzano, V. Gandin, D. Osella, M. Ravera, E. Gabano, J. A. Platts, E. Petruzzella, J. D. Hoeschele and G. Natile, *J. Med. Chem.*, 2012, **55**, 7182–92.

27 N. Margiotta, R. Ostuni, V. Gandin, C. Marzano, S. Piccinonna and G. Natile, *Dalton Trans.*, 2009, 10904–13.

28 R. A. Nadar, K. Farbod, K. C. der Schilden, L. Schlatt, B. Crone, N. Asokan, A. Curci, M. Brand, M. Bornhaeuser, M. Iafisco, N. Margiotta, U. Karst, S. Heskamp, O. C. Boerman, J. J. J. P. van den Beucken and S. C. G. Leeuwenburgh, *Sci. Rep.*, 2020, **10**, 5889.

29 R. A. Nadar, G. M. Franssen, N. W. M. Van Dijk, K. Codee-van der Schilden, M. de Weijert, E. Oosterwijk, M. Iafisco, N. Margiotta, S. Heskamp, J. J. J. P. van den Beucken and S. C. G. Leeuwenburgh, *Mater. Today Bio*, 2021, **9**, 100088.

30 F. Saad, D. M. Gleason, R. Murray, S. Tchekmedyian, P. Venner, L. Lacombe, J. L. Chin, J. J. Vinholes, J. A. Goas and M. Zheng, *JNCI J. Natl. Cancer Inst.*, 2004, **96**, 879–882.

31 L. Qiu, G. Lv, Y. Cao, L. Chen, H. Yang, S. Luo, M. Zou and J. Lin, *JBIC J. Biol. Inorg. Chem.*, 2015, **20**, 1263–1275.

32 L. Qiu, H. Yang, G. Lv, K. Li, G. Liu, W. Wang, S. Wang, X. Zhao, M. Xie and J. Lin, *Eur. J. Pharmacol.*, 2017, **810**, 120–127.

33 R. D. Feltham and R. G. Hayter, *J. Chem. Soc.*, 1964, 4587.

34 S. Savino, A. Toscano, R. Purgatorio, E. Profilo, A. Laghezza, P. Tortorella, M. Angelelli, S. Cellamare, R. Scala, D. Tricarico, C. M. T. Marobbio, F. Perna, P. Vitale, M. Agamennone, V. Dimiccoli, A. Tolomeo and A. Scilimati, *Eur. J. Med. Chem.*, 2018, **158**, 184–200.

35 D. SC., *Indian J Chem*, 1970, **8**, 193–194.

36 Kaleida Graph 3.5; Synergy software: Reading, PA, 2000

37 S. Piccinonna, N. Margiotta, C. Pacifico, A. Lopalco, N. Denora, S. Fedi, M. Corsini and G. Natile, *Dalt. Trans.*, 2012, **41**, 9689.

38 N. Margiotta, R. Ostuni, D. Teoli, M. Morpurgo, N. Realdon, B. Palazzo and G. Natile, *Dalt. Trans.*, 2007, 3131.

39 N. Margiotta, R. Ostuni, S. Piccinonna, G. Natile, I. Zanellato, C. D. Boidi, I. Bonarrigo and D. Osella, *J. Inorg. Biochem.*, 2011, **105**, 548–557.

40 N. Margiotta, F. Capitelli, R. Ostuni and G. Natile, *J. Inorg. Biochem.*, 2008, **102**, 2078–86.

41 M. Iafisco, B. Palazzo, M. Marchetti, N. Margiotta, R. Ostuni, G. Natile, M. Morpurgo, V. Gandin, C. Marzano and N. Roveri, *J. Mater. Chem.*, 2009, **19**, 8385.

42 C. J. P. A. V. Naumkin, A. Kraut-Vass, S.W. Gaarenstroom, .

43 K. Matsumoto, K. Sakai, K. Nishio, Y. Tokisue, R. Ito, T. Nishide and Y. Shichi, *J. Am. Chem. Soc.*, 1992, **114**, 8110–8118.

44 A. Dolmella, F. P. Intini, C. Pacifico, G. Padovano and G. Natile, *Polyhedron*, 2002, **21**, 275–280.

45 D. Corinti, G. Frison, B. Chiavarino, E. Gabano, D. Osella, M. E. Crestoni and S. Fornarini, *Angew. Chemie Int. Ed.*, 2020, **59**, 15595–15598.

46 G. Bandoli, P. A. Caputo, F. P. Intini, M. F. Sivo and G. Natile, *J. Am. Chem. Soc.*, 1997, **119**, 10370–10376.

47 A. Barbanente, R. M. Iacobazzi, A. Azzariti, J. D. Hoeschele, N. Denora, P. Papadia, C. Pacifico, G. Natile and N. Margiotta, *Molecules*, 2021, **26**, 3417.

ARTICLE